Effect of Side Chain Structure on the Conformation of Poly(*N*-propargylalkylamide)

Ryoji Nomura,* Junichi Tabei, and Toshio Masuda*

Department of Polymer Chemistry, Graduate School of Engineering, Kyoto University, Kyoto 606-8501, Japan

Received October 1, 2001

ABSTRACT: Achiral *N*-propargylalkylamides (**1a**−**1g**, HC≡CCH_2NHR) having various alkyl groups (R = CH_3, C_2H_5, C_3H_7, *i*-C_3H_7, *i*-C_4H_9, *n*-C_5H_{11}, *n*-C_7H_{15}) were homopolymerized or copolymerized with a chiral comonomer, (*R*)-*N*-propargyl-3,7-dimethyloctanamide (**2**), in the presence of a Rh initiator to establish the relationship between the main-chain conformation and the structure of the pedant groups. ^{1}H NMR and viscosity measurements of the homopolymers revealed that the structure of the pendant groups markedly influences the rigidity of the polymer backbone and the stability of the helical conformation. The copolymerization using the achiral comonomers having linear or α-branched alkyl groups showed poor or no cooperative effects on the helical conformation, meaning that these polymers exist in a disordered state. On the other hand, a stable helical conformation, i.e., a long persistence length of the helical domain, was attainable for the polymer having *β*-branched alkyl chains (poly(**1e**), R = *i*-C_4H_9), which was evidenced by a clear, positive nonlinear relationship between the feed ratio of **1e** to **2** and the optical rotation of the copolymers. UV−visible spectroscopic studies demonstrated that, in $CHCl_3$, the helical and disordered main chains display absorption centered at 400 and 320 nm, respectively, which resulted in different colors in solution of the helical (yellow) and disordered (achromic) polymers. Thermochromism was achieved by the thermally induced reversible conformational change between helical and disordered states. The thermodynamic parameters (ΔG_r, ΔH_r, and ΔS_r) that govern the stability of the helical conformation of a copolymer were estimated by the temperature dependence of the populations of the helical and disordered states using UV−visible spectra.

Introduction

Natural biopolymers, such as protein[1] and DNA,[2] frequently have helical conformations. These three-dimensionally ordered structures contribute significantly to the specific functions that maintain the living systems. Advances in polymer synthesis have produced a variety of well-ordered helical polymers,[3] including polyisocyanates,[4] polyisocyanides,[5] polychloral,[6] poly(alkyl methacrylates) with bulky substituents,[7] polysilanes,[8] polyacetylenes,[9,10] and polythiophenes.[11] These helical polymers possess rigid or semiflexible main chains, which contributes to the stability of their helical conformation. On the other hand, polymers with flexible backbones cannot maintain a helical conformation in solution. Induction of a helical conformation in flexible polymers uses very bulky pendant groups that stiffen the backbone due to their steric repulsion. For example, poly(triphenylmethyl methacrylate) has a stable helical conformation, while poly(methyl methacrylate) is randomly coiled in solution.[7] Thus, synthetic polymers utilize only van der Waals interactions for induction of the helical conformation.

In contrast, the conformation of biopolymers, such as α-helical polypeptides, is induced and stabilized by both hydrogen bonds and van der Waals interactions. Particularly, well-arranged intramolecular and/or intermolecular hydrogen bonds contribute significantly to the secondary conformation. Unfortunately, the arrangement of hydrogen bonds in synthetic macromolecules is very difficult except for synthetic DNAs and polypeptides. Only a few examples have been demonstrated so far,[12−14] in which the hydrogen bond plays a very important role for the secondary structure of several synthetic polymers.

Scheme 1

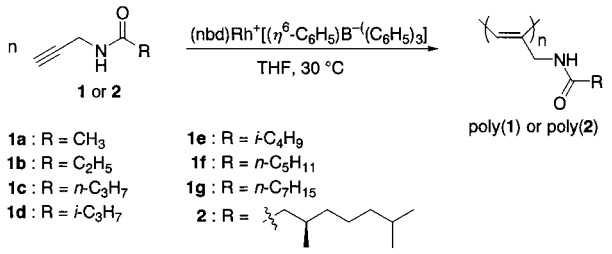

This background motivated us to synthesize polymers with biomimetically stabilized helical conformation, and we recently reported that, by construction of intramolecular hydrogen bends between the pendant groups, a helical conformation can be induced to substituted polyacetylene.[15] Generally, the polymers from monosubstituted aliphatic 1-alkynes are too flexible to adopt a helical conformation unless they have very bulky substituents.[16] However, a poly(*N*-propargylalkylamide), poly(**2**), which has chiral substituents linked by the amide groups, possesses a semiflexible main chain and exists in a helical conformation with an excess of one-handed screw sense (Scheme 1). This helix preference of poly(**2**) is contributed by the hydrogen bonds that were spectroscopically evidenced to be intramolecularly located between the pendant amide groups.[15]

Since the intensity of chiroptical properties of poly(**2**) reversibly changes with temperature,[15] the helical conformation of poly(*N*-propargylalkylamides) in solution is dynamic. Like polyisocyanates, polysilanes, poly(propiolic esters), poly(*N*-propargylalkylamides) readily undergo the helix−helix and/or helix−random coil tran-

* Corresponding author. Telephone: +81-75-753-5613. Fax: +81-75-753-5908. E-mail: masuda@adv.polym.kyoto-u.ac.jp.

10.1021/ma0117155 CCC: $22.00
Published on Web 03/08/2002

Table 1. Homopolymerization of *N*-propargylalkylamides (1 and 2) Having Various Substituents

monomer	yield (%)	M_n[a]	M_w/M_n[a]	$\nu_{1/2}$[b] (Hz) vinyl	$\nu_{1/2}$[b] (Hz) N−H	α[c]
1a	99[d]	7100[e]	9.96[e]			
1b	89[d]	10000	1.44	11	20	
1c	90[d]	8700	2.14	12	24	
1d	51[d]	8700	2.23			0.74
1e	86[f]	9500	1.66			0.83
1f	77[g]	18000	2.24	30	69	0.76 (0.98)
1g	63[g]	14000	1.26	33	58	
2	62[g]	8100	1.68	98		0.91

[a] Estimated by GPC (THF, PSt standards). [b] Half-height line widths of ^{1}H NMR resonance in $CDCl_3$ at 19 °C. [c] Viscosity index in THF at 40 °C. The value in parentheses was measured in THF at 30 °C. [d] Ether-insoluble part. [e] Water-soluble part. Estimated by GPC (H_2O, PEO standards). [f] Hexane-insoluble part. [g] Methanol-insoluble part.

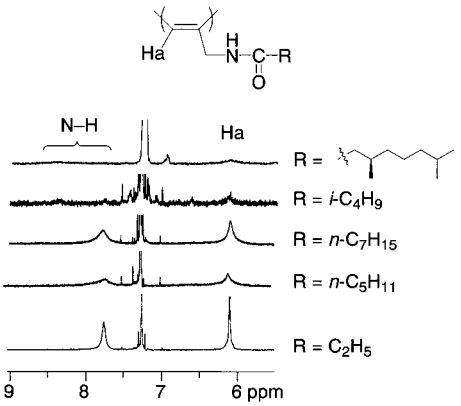

Figure 1. The ^{1}H NMR spectra of poly(**1b**), poly(**1e**), poly(**1f**), poly(**1g**), and poly(**2**) in $CDCl_3$ at 19 °C.

sition in solution. Thus, an individual polymer chain contains both helical and disordered domains, and the stability of the helical conformation, i.e., the population of the helical state, depends on the free energy difference (ΔG_r) between the helical and disordered, randomly coiled conformations.[17] In the present study, we focused on the effects of the side chain structure on the stability of the helical conformation of poly(*N*-propargylalkylamides). To explore these effects, we copolymerized various *N*-propargylalkylamides (**1a**−**1g**) with a chiral comonomer, (*R*)-*N*-propargyl-3,7-dimethyloctanamide (**2**). Such chiral/achiral copolymerization allows elucidation of the helix stability.[18] We also studied in detail the UV−visible spectroscopy of the resultant copolymers and homopolymers, which led to a finding that a simple UV−visible spectroscopic technique allows distinction between the helical and disordered states. By using the UV−visible spectra, we determined the thermodynamic parameters governing the stability of the helical conformation, by which the profile of the helical conformation of poly(*N*-propargylalkylamide) is discussed.

Results and Discussion

Homopolymers of Various *N*-Propargylalkylamides. The monomers (**1** and **2**) examined in the present study are illustrated in Scheme 1. The homopolymerization was carried out in the presence of a Rh complex, (nbd)Rh$^+$[(η^6-C_6H_5)B$^-$(C_6H_5)$_3$][19] (nbd = 2,5-norbornadiene), because Rh initiators give good yields of substituted polyacetylenes with excellent cis−transoidal stereoregularity[16] and because the stereoregulation to the cis geometrical main-chain structure is indispensable for the construction of helical substituted polyacetylenes.[10] Table 1 tabulates the results of the homopolymerization. Although the polymerization was conducted for 1 h, the polymerization is likely to be completed within a few minutes: the addition of the monomer to the initiator solution resulted in a rapid increase in the viscosity and temperature of the polymerization solution. The homopolymer from **1a** was insoluble in organic solvents and partly (ca. 80%) soluble in water and methanol. Poly(**1b**) also partly dissolved in water and showed high solubility in a variety of solvents including $CHCl_3$, THF, methanol, DMF, and DMSO. Generally, the polymers with short alkyl chains such as poly(**1b**), poly(**1c**), poly(**1d**), and poly(**1e**) dissolved well in both polar and nonpolar solvents, and those having long alkyl chains were soluble in nonpolar solvents. The solubility of the homopolymers is summarized in the Supporting Information. Attempts to prepare polymers having very long linear alkyl chains such as *n*-C_9H_{19} and *n*-$C_{11}H_{23}$ groups resulted in insoluble polymers. Polymers having a branched structure at the β-position to the carbonyl group [poly(**1e**) and poly(**2**)] gave a bright yellow solution in $CHCl_3$, while the diluted $CHCl_3$ solutions of the other homopolymers were almost achromic.

The effects of the pendant groups of poly(*N*-propargylalkylamide) were first recognized in their ^{1}H NMR spectra. The ^{1}H NMR spectra (expanded) of several homopolymers [poly(**1b**), poly(**1e**), poly(**1f**), poly(**1g**), and poly(**2**)] in $CDCl_3$, and some peak assignments are illustrated in Figure 1. As seen in Figure 1, a slight structural variation in the side chain caused a pronounced change in the mobility, i.e., the flexibility of the main chain. For example, poly(**1b**), having short linear pendant groups, displayed clear signals even at low temperature (19 °C), indicating its high main-chain mobility. In a similar way, well-resolved ^{1}H NMR peaks were observed for poly(**1c**). Cis−transoidal stereoregular-substituted polyacetylenes obtained with Rh initiators exhibit well-resolved signals attributed to the vinyl proton around 6−7 ppm.[16c] Thus, a reasonable peak assignment is possible as illustrated in Figure 1a. Comparison of the integrated intensity of the vinyl and NCH_2 peaks concluded that the cis stereoregularities of poly(**1b**) and poly(**1c**) were quantitative.[20] On the other hand, the peaks of the protons close to the main chain were very broad for the polymers having long linear side chains [poly(**1f**) and poly(**1g**)]. The half-height line widths ($\nu_{1/2}$) of the vinyl and N−H protons of these polymers were much larger than those of poly(**1b**) and poly(**1c**) (Table 1). However, the ^{1}H NMR spectra of these polymers at high temperature (55 °C) provided well-resolved signals attributed to all of the protons,[15] and the cis stereoregularity was confirmed to be quantitative using the ^{1}H NMR spectra. Thus, the broadening of the NMR resonance of poly(**1f**) and poly(**1g**) at 19 °C is due not to the lower stereoregulation but to the limited mobility of their main chain. Introduction of a branch at the position β to the carbonyl group more significantly rigidifies the polymer backbone. For example, the N−H and vinyl protons of poly(**1e**) cannot be clearly detected at 19 °C as shown in Figure 1, and well-resolved resonances were not attainable even at 55 °C. Similarly, the half-height line width of the vinyl proton of poly(**2**), which possesses long alkyl chains with a β-branched structure, was almost 1 order of magnitude larger than that of poly(**1b**) (Table 1), and

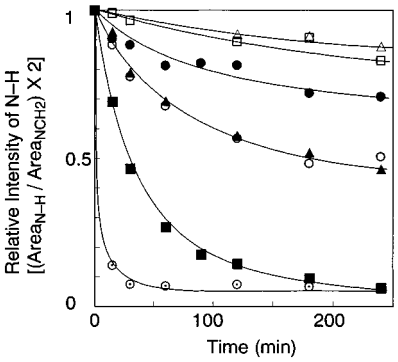

Figure 2. Time dependence of the relative intensity of the N−H protons to the vinyl protons for (○) monomer **1c**, (■) poly(**1b**), (○) poly(**1d**), (□) poly(**1e**), (▲) poly(**1f**), (●) poly(**1g**), and (△) poly(**2**) in a mixed solvent ($CDCl_3/CD_3OD$ = 90/10 wt/wt) at 20 °C. The polymer concentrations were 200 mM (monomer unit).

the ^{1}H NMR measured at 60 °C showed broadened signals.[21] These results mean that the main chain of poly(**1e**) and poly(**2**) is stiffer than that of the other polymers carrying linear or α-branched side chains, thus contributing to the thermal stability of the helical conformation of poly(**2**).[15]

Using the viscosity index (α) of $[\eta] = \kappa M^{\alpha}$ in the Mark−Hauwink−Sakurada plot, where $[\eta]$ is the intrinsic viscosity and M is the absolute molecular weight based on the universal calibration curve, the rigidity of the polymer backbone can be discussed in detail. The viscosity indexes of the polymers (Table 1) were measured at 40 °C owing to the unsatisfactory solubility of poly(**1c**), poly(**1e**), and poly(**2**) at 30 °C. The α value of poly(**1f**) at 40 °C (0.76) may convince one that it possesses a flexible main chain.[22] However, as described below, the conformation of poly(*N*-propargylalkylamides) is very sensitive to temperature because of the very large entropy loss for the transition from the disordered to the helical conformation. Hence, the helical conformation rapidly decomposes by thermal stimuli. Indeed, the viscosity index of poly(**1f**) at 30 °C (0.98) is much larger than that at 40 °C, which means that poly(**1f**) is a semiflexible polymer below 30 °C.[22] It is interesting that the introduction of a branched structure to the position β of the carbonyl group is effective to rigidify the polymer backbone. Specifically, although the α value of poly(**1d**) (0.76) having *i*-Pr units was almost the same as that of poly(**1f**), poly(**1e**) bearing *i*-Bu groups exhibited a large value (0.83). The polymer from **2**, which has a β-branched, long alkyl chain, showed higher α value than other polymers. The data based on the ^{1}H NMR and viscosity measurements reveal that the rigidity of poly(*N*-propargylalkylamide) increases by increasing the length of the alkyl chain and introducing a branch to the β-position of the carbonyl group.

The effects of the structure of the pendant groups were also found in the rate of the H−D exchange reaction of the amide proton. For example, the amide protons in the homopolymers having short alkyl side chains [poly(**1b**)] were substituted by deuteriums almost completely in a $CDCl_3-CD_3OD$ mixed solvent ($CDCl_3/CD_3OD$ = 90/10 wt/wt) within 3 h (Figure 2). On the other hand, this reaction was apparently slow for the polymers with long linear alkyl side chains [poly(**1f**) and poly(**1g**)]. Furthermore, only 10% of the protons were replaced for the polymers [poly(**1e**) and poly(**2**)] having

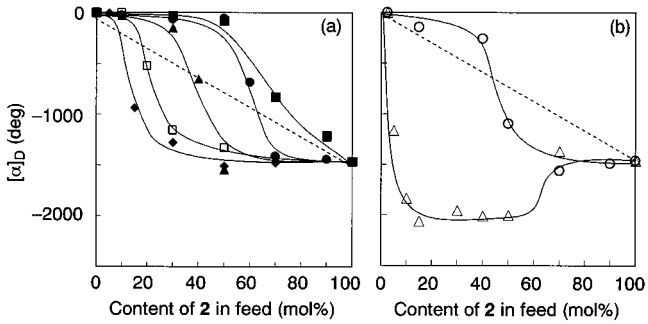

Figure 3. Plot of the optical rotation of (a) (■) poly(**1a**-*co*-**2**), (●) poly(**1b**-*co*-**2**), (▲) poly(**1c**-*co*-**2**), (◆) poly(**1f**-*co*-**2**), and (□) poly(**1g**-*co*-**2**) and (b) (○) poly(**1d**-*co*-**2**) and (△) poly(**1e**-*co*-**2**) against the feed content of monomer **2** (in $CHCl_3$ at room temperature).

a β-branched structure on this time scale. All of the homopolymers showed the amide I absorption at 1637 cm^{-1} in $CHCl_3$, and no absorption attributed to the free amide group was detected. In a similar way, only hydrogen bonded N−H frequency was detected in the IR spectra for all of the homopolymers. This indicates that the side chain amide groups exist in an aggregated form irrespective of the side-chain structure. Thus, introduction of the β-branching structure is enough to shield the hydrogen-bonded amide groups from the solvents and consequentially to stabilize the hydrogen bond.

Copolymerization. To estimate the stability of the helical conformation of poly(*N*-propargylalkylamide), the achiral and chiral comonomers **1** and **2**, were copolymerized under similar conditions as for the homopolymerization. The results of the copolymerizations are summarized in Table 2 in the Supporting Information. All of the copolymers were soluble in common organic solvents, except for poly(**1a**-*co*-**2**) having low feed content of **2**.[23]

Figure 3 plots the optical rotation of the copolymers against the feed content of **2**. The optical rotation is amplified in polymers with a stable helical conformation, that is, a large population of the helical domain and hence very low frequency of helix reversal. Introduction of a small amount of a chiral segment can provide an excess of one-handed screw sense and, consequently, very large chiroptical properties. Therefore, the chiroptical properties and the content of a chiral segment have a positive nonlinear relationship. In contrast, if the helical conformation is unstable, the chiroptical properties of the chiral/achiral copolymers should be identical to or lower than those linearly calculated from the chiral comonomer content.

As shown in Figure 3, the dependence of the chiroptical properties of chiral/achiral copolymers on the feed ratio was strongly influenced by the structure of the pendant groups. For instance, in the case of less hindered comonomer **1a**, no chiral amplification was recognized. On the other hand, the copolymerization using linear alkyl pendants longer than the methyl group displayed the chiral amplification phenomenon to some extent. For example, when the feed content of chiral comonomer **2** was high (70−80%), the copolymers with **1b** showed optical rotations ($[\alpha]_D$) that are much larger than the value linearly calculated from the feed ratio of the comonomers. However, a further decrease in the feed content of **2** caused a steep decrease in the optical rotation, and almost no chirality was detected

for poly(**1b**-*co*-**2**) when the feed content of **2** was below 50%. When comonomers (**1f** and **1g**) having longer alkyl groups were employed, the copolymers maintained their rich chiroptical properties even at a low feed content of **2**. However, even these copolymers also lacked chirality when the feed content of **2** was lower than 10%. The α-branched comonomer **1d**, behaved similarly (Figure 3b). In contrast, the copolymers derived from **1e** bearing a *β*-branched alkyl chain clearly displayed a positive, nonlinear relationship between the optical rotation and the feed ratio. A very large optical rotation (ca. −2000°) that is much larger than that of poly(**2**) was attainable when the feed content of **2** was 15−50%. Even a 5% feed of the comonomer **2** produced a copolymer having a quite large optical rotation (−1160°) (the reason for the larger chiroptical properties of poly(**1e**-*co*-**2**) (**1e**/**2** = 10/90−50/50 in feed) than that of poly(**2**) is discussed below).

These data lead to the following conclusions. The increase in the side-chain length enhances the persistence length of the helical domain. However, linear alkyl side chains are not bulky enough to maintain the helical conformation even if their length is extended. Introduction of the branched structure at the α carbon is also inadequate for the construction of a stable helical conformation although *i*-Pr groups are apparently bulkier than linear alkyl chains. Thus, monomers **1a**−**1d**, **1f**, and **1g** bearing linear or α-branched alkyl chains give disordered, randomly coiled main chains. However, the copolymers based on these comonomers showed very large optical rotation in the case of the high feed content of **2** that has a *β*-branched alkyl chain. Thus, polymers having *β*-branched alkyl chains adopt a helical conformation with a long persistence length. This idea is supported by the nonlinear effect on the copolymerization of **1e** with **2**. As described above, the side chain significantly affects the stability of the hydrogen bonds constructed between the side chains, and the hydrogen-bonds in poly(**1e**) and poly(**2**) are considerably stable compared with those of polymers bearing linear or α-branched side chains. Therefore, the highly stabilized hydrogen bonds for poly(**1e**) and poly(**2**) enhance the main-chain rigidity and the stability of the helical conformation. This means that both van der Waals interactions and hydrogen bonds stabilize the helical conformation. However, as demonstrated below, even the copolymers based on monomer **1e** as well as poly(**2**) were not able to stay in the helical conformation in solvents than can hydrogen bond with amide groups; no CD effects were observed for poly(**2**) in methanol, DMF, and THF. This means that, without the contribution of the hydrogen bond, the van der Waals interactions alone cannot induce the helical conformation. Thus, as with biopolymers, hydrogen bonds and van der Waals interactions control the conformation of poly(*N*-propargylalkylamides).

UV−Visible Spectroscopic Study. The UV−visible spectroscopy of poly(*N*-propargylalkylamides) provided very unique and important information on the polymer conformation. As an example, the UV−visible spectra of poly(**1d**), poly(**1d**-*co*-**2**) (**1d**/**2** = 50/50 in feed), poly(**1e**), and poly(**2**) are illustrated in Figure 4. As discussed in the previous section, poly(**1d**) exists in a randomly coiled state. This polymer displayed an absorption centered at 320 nm. In contrast, the absorption of poly(**1e**) and poly(**2**) which adopt a helical structure was located at 400 nm, and these polymers showed no absorption maximum around 320 nm. In the case of the

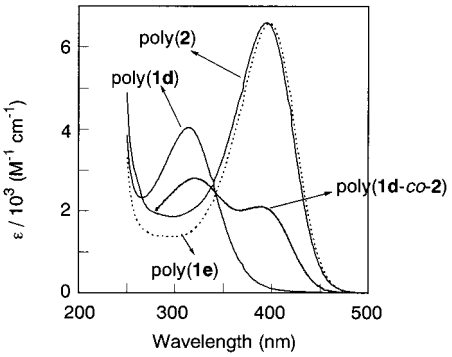

Figure 4. UV−visible spectra of poly(**1d**), poly(**1d**-*co*-**2**) (**1d**/**2** = 50/50 in feed), poly(**1e**), and poly(**2**) in $CHCl_3$ at room temperature.

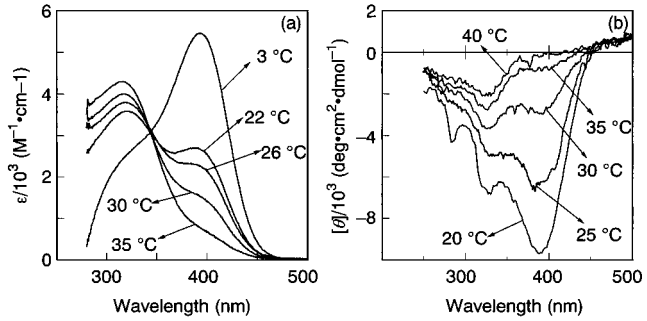

Figure 5. Temperature-variable (a) UV and (b) CD spectra of poly(**1d**-*co*-**2**) (**1d**/**2** = 50/50 in feed) in $CHCl_3$.

copolymer ($[\alpha]_D$ = −1100°), both absorptions were detected. This phenomenon might be explained hypothetically that the segment derived from monomer **1d** simply shows an absorption at 320 nm and the units of **1e** and **2** absorb 400 nm light. However, this hypothesis can be readily ruled out by the following observations. First, the peak intensity ratio of the copolymers of **1d** with **2** disagreed with the feed ratio of these comonomers. Second, a copolymer, poly(**1d**-*co*-**2**) (**1d**/**2** = 30/70 in feed), which possesses a very large optical rotation (−1410°) comparable to that of poly(**2**), exhibited only one absorption at 400 nm. Finally, clearer evidence is the fact that a change in temperature yielded a drastic change in the UV−visible spectrum of the copolymer, poly(**1d**-*co*-**2**) (**1d**/**2** = 50/50 in feed). For example, as shown in Figure 5a, the decrease in temperature amplified the absorption at 400 nm, simultaneously decreasing the intensity of the absorption located at 320 nm. An isosbestic point was observed upon this temperature change, and this thermally induced process was reversible; the magnitude of the absorption at 400 nm decreased and that at 320 nm increased when the temperature was increased. The absorption located at 400 nm therefore originates from the helical main-chain chromophore and the other absorption around 320 nm is due to the main-chain absorption in the disordered state. The temperature dependence of the UV−visible spectrum is explained by the increasing population of the helical domain with decreasing temperature, which is supported by the temperature-variable CD spectra. As shown in Figure 5b, the magnitude of the Cotton effect changed reversibly with temperature; decreasing and increasing temperature increased and decreased the intensity of the CD spectra, respectively. Therefore, Figure 5a demonstrates that poly(**1d**-*co*-**2**) (**1d**/**2** = 50/50 in feed) exists predominantly in a helical conformation at 3 °C, and adopts a disordered conformation at

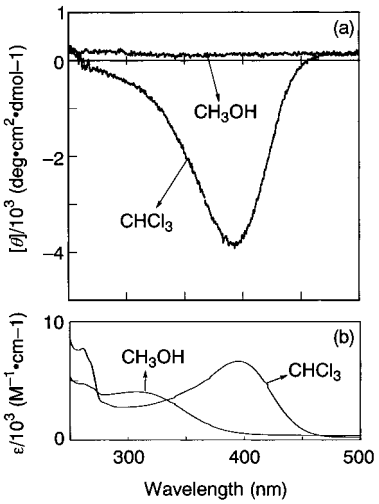

Figure 6. (a) CD and (b) UV−visible spectra of poly(**1e**-*co*-**2**) (**1e**/**2** = 90/10 in feed) in methanol and $CHCl_3$.

35 °C. This drastic conformational change takes place in a very small temperature range (ca. 30 K). The marked change in the viscosity index (α) of poly(**1f**) with a small change in temperature (Table 1) is evidently due to this thermally induced, drastic conformational change.

This spectral change upon the temperature is accompanied by a change in the color of the polymer solution. For example, a dilute $CHCl_3$ solution of a copolymer, poly(**1d**-*co*-**2**) (**1d**/**2** = 50/50 in feed), was colorless at room temperature, but yellow in an ice-bath. Poly(**1f**) and poly(**1e**) changed color between achromic and yellow; a colorless solution of poly(**1f**) turned yellow on cooling and lost its color reversibly on standing at room temperature. A yellow solution of poly(**1e**) at room temperature became achromic on heating but gradually recovered its original yellow color when the heating was stopped.[24] Hence, poly(*N*-propargylalkylamide) is thermochromic, which is driven by the conformational change between a helix and a random coil.

Poly(*N*-propargylalkylamides) also achieved a solvatochromism. An example is clearly demonstrated in Figure 6, where the solvent-driven conformational change occurs. In $CHCl_3$, poly(**1e**-*co*-**2**) (**1e**/**2** = 90/10) exhibited a large optical rotation ($[\alpha]_D = -2060°$), intense CD effects, and an absorption around 400 nm. In contrast, this copolymer showed no CD effects and absorbed 320 nm light in methanol, which corresponded to its achromatic methanol solution.

The above-mentioned assignment of the UV−visible absorption provides a plausible reason for the larger optical rotation of poly(**1e**-*co*-**2**) (**1e**/**2** = 10/90−50/50 in feed) than that of poly(**2**). These copolymers and poly(**2**) exhibited identical UV−visible spectral patterns with only one absorption at 400 nm. Therefore, both polymers possess a high population of the helical structure, and the content of the disordered state is negligibly small. Therefore, the lower chiroptical property of poly(**2**) can be explained by its unsatisfactorily biased screw sense. As demonstrated in our previous paper, stereoregular cis−transoidal poly(propiolic esters) with chiral side chains can undergo a helix inversion by changing either the temperature or solvent.[25] In particular, the helix inversion occurs readily for the polymers having a long alkyl side chain. Thus, poly(**2**) that has long alkyl groups may prefer the helix inversion more than poly(**1e**). The sparingly populated, opposite screw sense probably contributes to the poorer optical rotation of poly(**2**) than that of poly(**1e**).

Thermodynamics of the Helical Conformation. As mentioned above, poly(**1e**) and poly(**2**) possess a high population of the helical domain and a negligible amount of the disordered state, while the other homopolymers are randomly coiled. The intensity of the absorption at 400 nm for poly(**1e**) did not change when the temperature was below 30 °C. The absorption coefficients of the disordered and helical conformations were, thus, readily calculated to be 4040 and 6600 $M^{-1}\cdot cm^{-1}$, respectively. From the temperature-variable UV−visible spectra, the temperature dependence of the ratio of the helical to the disordered states was estimated, which allowed the determination of the thermodynamic parameters that govern the helix stability. The free energy difference between the helical and disordered states, ΔG_r,[17] can be defined as

$$\Delta G_r = -RT \ln K$$

where K is the equilibrium constant for the transition process from the disordered to the helical conformation. The proportion of the helical to the disordered state determines the constant K. Thus, the constant K is given by

$$K = N_h/N_r$$

where N_h is the number of monomer units which exist in a helical conformation and, similarly, N_r is defined as the number of monomer units in the disordered state. N_h and N_r are readily provided by the computational deconvolutions of the UV−visible spectra. The thermodynamic theory predicts

$$-R \ln K = \Delta H_r/T - \Delta S_r$$

where ΔH_r and ΔS_r are the enthalpy and entropy changes upon the transition from the disordered to the helical state. The plot of $-R \ln K$ against the reciprocal of temperature gave ΔH_r and ΔS_r. As an example, ΔH_r and ΔS_r of poly(**1d**-*co*-**2**) (**1d**/**2** = 50/50 in feed) were calculated to be -15.2 ± 1.44 kcal/mol and -54.4 ± 5.17 cal/mol·K.[26] Emphasis should be placed on these very large, negatively signed entropy and enthalpy changes. To the best of our knowledge, this is the first example of the determination of ΔH_r and ΔS_r for the transition process from the randomly coiled to a helical conformation of an artificial polymer.

Here, the secondary structure of stereoregular substituted polyacetylenes can be roughly but simply pictured by the function of the dihedral angle of the single bonds.[25] The entropy difference, ΔS_r, relates to the probability of encountering the helical conformation, i.e., the relative range of the dihedral angle allowed for giving the helical conformation. Semiflexible or rigid substituted polyacetylenes should originally possess a limited region of the dihedral angle available, which consequentially yields a relatively high probability of the conformation representing the helical backbone. Indeed, the entropy and enthalpy losses for semiflexible poly(hexyl propiolate) (the viscosity index, $\alpha = 1.2$ in THF at 30 °C),[27] determined by ^1H NMR,[28] were as small as -0.73 ± 0.058 cal/mol·K and -1.74 ± 0.14 kcal/mol, respectively. On the other hand, for substituted polyacetylenes with a flexible main chain such as the polymers from monosubstituted aliphatic acetylenes, a

wide region of the dihedral angle about the single bond is allowed. The large entropy loss for poly(*N*-propargylalkylamides) is, thus, explained by the low probability of encountering the region of the dihedral angle which offers the helical conformation. To give the helical backbone, this large, negatively signed entropy change is compensated by the negatively large enthalpy change. In other words, bonding energy should be provided to overcome the large entropy loss. In the present system, the binding energy is given not only by the van der Waals interaction but also by the hydrogen bond. This situation is identical to that of the folding process of proteins where the large entropy and binding energy contributions are well-balanced.[1]

Conclusion

The stability of the helical conformation of poly(*N*-propargylalkylamide) was explored by the homopolymerization of various achiral monomers and their copolymerizations with a chiral comonomer. A slight structural change of the pendant groups significantly influenced the rigidity of the backbone, the stability of the hydrogen bond and the helical conformation. Although the polymers with linear or α-branched alkyl side chains cannot exist in a helical conformation at ambient temperature, introduction of a branched structure at the *β*-carbon produces a helical conformation with a large helical domain size. However, even the polymers with *β*-branched side chains exist in the disordered state in the absence of the hydrogen-bond contribution. Thus, the conformation of poly(*N*-propargylalkylamides) is strongly influenced by hydrogen bonds and van der Waals interactions. Like the melting process of biopolymers, the polymers readily undergo a helix−random coil transition by reducing the contributions of the noncovalent interactions, which is induced by external stimuli such as a change in temperature and solvents. This conformational change is accompanied by a change in the UV−visible spectra. The polymers show thermochromism and solvatochromism upon the change of the conformation. The population of the helical and the disordered states can be calculated by the UV−visible spectra, which allows estimation of the thermodynamic parameters that determine the profile of the helix. These parameters clearly demonstrated the significant contribution of the noncovalent interactions to stabilization of the helical conformation of poly(*N*-propargylalkylamides).

Experimental Section

General Data. The molecular weights and polydispersities of the polymers were determined by using gel permeation chromatography (eluent, chloroform; Shodex columns K804, K805, and K806; calibrated by polystyrene standards). For poly(**1a**), GPC measurements were carried out using a Tosoh column TSK−Gel α-M, and the sample was eluted with water. The molecular weight and polydispersity of poly(**1a**) were estimated based on poly(ethylene glycol) standards. The measurement of viscosity indexes was conducted at the NTT Basic Research Laboratories or the Tokyo Institute of Technology using GPC apparatuses with a Viscotec T60A viscometer (eluent, THF). ^{1}H NMR spectra were recorded with a JEOL EX-400 spectrometer. CD spectra were measured in a quartz cell (thickness 1 cm) using a Jasco J600 spectropolarimeter. Specific rotations were determined with a Jasco DIP-1000 spectropolarimeter. UV−visible and IR spectra were recorded with Jasco V-550 and Shimadzu FTIR-8100 spectrophotometers, respectively. Melting points were measured on a Yanaco micro melting point apparatus and were not corrected. Elemental analyses were carried out using Yanaco CHN Corders MD-2, MD-3, MD-5, and MD-6. Mass spectra were obtained on a JEOL SX-102A instrument. THF was distilled from Na/benzophenone under nitrogen. Other solvents and reagents were used as received. (nbd)Rh$^+$[(η^6-C_6H_5)B$^-$(C_6H_5)$_3$] was prepared according to the literature.[19a] (*R*)-3,7-Dimethyloctanoic acid was prepared by the hydrogenation of (*R*)-citronellic acid in the presence of Pd/C.[29] The monomers were prepared by the condensation of the corresponding acyl chlorides with propargylamine in the presence of pyridine in ether. Purification of the monomers was carried out by the SiO_2 column chromatography (eluent; hexane/ethyl acetate). Further purification was conducted by recrystallization from hexane. Spectral data for new compounds were as follows.

***N*-Propargylacetoamide (1a).** Yield: 39%; a white solid, mp 90−91 °C. ^{1}H NMR ($CDCl_3$, 400 MHz): δ 2.03 (s, 3H), 2.24 (s, 1H), 4.04 (s, 2H), 6.20 (s, 1H). ^{13}C NMR ($CDCl_3$, 100 MHz): δ 22.78, 28.99, 71.17, 79.54, 170.20. IR (KBr): 3227, 3083, 2116, 1637, 1569, 1302, 1253, 1097, 1028, 719 cm^{-1}. Anal. Calcd for C_5H_7NO: C, 61.86; H, 7.22; N, 14.43. Found: C, 61.72; H, 7.24; N, 14.36.

***N*-Propargylpropanamide (1b).** Yield: 89%; a white solid, mp 59−61 °C. ^{1}H NMR ($CDCl_3$, 400 MHz): δ 1.17 (t, 3H, J = 8.0 Hz), 2.25 (q, 2H, J = 8.0 Hz), 2.23 (d, 1H, J = 2.4 Hz), 4.05 (dd, 2H, J = 2.4, 5.4 Hz), 5.93 (s, 1H). ^{13}C NMR ($CDCl_3$, 100 MHz): δ 9.57, 29.06, 29.32, 71.38, 79.61, 173.41. IR (KBr): 3236, 3038, 2108, 1637, 1541, 1419, 1242, 1030, 708 cm^{-1}. MS (EI): *m/e* 111 M$^+$.

***N*-Propargylbutanamide (1c).** Yield: 97%; a white solid, mp 31−32 °C. ^{1}H NMR ($CDCl_3$, 400 MHz): δ 0.95 (t, 3H, J = 6.3 Hz), 1.62−1.69 (m, 2H), 2.17 (t, 2H, J = 7.3 Hz), 2.22 (d, 1H, J = 2.4 Hz), 4.05 (dd, 2H, J = 2.4, 5.4 Hz), 5.71 (s, 1H). ^{13}C NMR ($CDCl_3$, 100 MHz): δ 13.68, 18.95, 29.06, 38.32, 71.45, 79.61, 172.61. IR (KBr): 3250, 2963, 1626, 1541, 1429, 1240, 891, 677, 542 cm^{-1}. HRMS: calcd for $C_7H_{11}NO$ (*m/z*), 125.0841; found, 125.0840.

***N*-Propargyl-2-methylpropanamide (1d).** Yield: 92%; a white solid, mp 68−70 °C. ^{1}H NMR ($CDCl_3$, 400 MHz): δ 1.16 (d, 6H, J = 6.8 Hz), 2.22 (t, 1H, J = 2.5 Hz), 2.37 (h, 1H, J = 6.8 Hz), 4.04 (dd, 2H, J = 2.5, 5.4 Hz), 5.66 (s, 1H). ^{13}C NMR ($CDCl_3$, 100 MHz): δ 19.42, 29.14, 35.41, 71.65, 79.67, 176.46. IR (KBr): 3324, 2974, 2163, 1635, 1541, 1238, 1105, 846, 544 cm^{-1}. HRMS: calcd for $C_7H_{11}NO$ (*m/z*), 125.0841; found, 125.0841.

***N*-Propargyl-3-methylbutanamide (1e).** Yield: 86%; a white solid, mp 45−46 °C. ^{1}H NMR ($CDCl_3$, 400 MHz): δ 0.95 (d, 6H, J = 6.3 Hz), 2.06−2.22 (m, 4H), 4.05 (dd, 2H, J = 2.4, 5.4 Hz), 5.65 (s, 1H). ^{13}C NMR ($CDCl_3$, 100 MHz): δ 22.42, 26.15, 29.06, 45.74, 71.49, 79.56, 172.13. IR (KBr): 3229, 2989, 2118, 1637, 1546, 1421, 1248, 1030, 721 cm^{-1}. HRMS: calcd for $C_8H_{13}NO$ (*m/z*), 139.0997; found, 139.0997.

***N*-Propargyloctanamide (1g).** Yield: 68%; a white solid, mp 72−73 °C. ^{1}H NMR ($CDCl_3$, 400 MHz): δ 0.88 (t, 3H, J = 6.8 Hz), 1.19−1.28 (m, 8H), 1.61−1.69 (m, 2H), 2.20 (t, 2H, J = 7.8 Hz), 2.24 (t, 1H, J = 2.8 Hz), 4.04 (dd, 2H, J = 2.8, 5.3 Hz), 5.68 (s, 1H). ^{13}C NMR ($CDCl_3$, 100 MHz): δ 13.74, 22.30, 25.20, 28.64, 28.79, 28.84, 31.31, 36.14, 71.20, 79.28, 172.25. IR (KBr): 3292, 3146, 1637, 1541, 1458, 698 cm^{-1}. HRMS: calcd for $C_{11}H_{19}NO$ (*m/z*), 181.1467; found, 181.1466.

(*R*)-*N*-Propargyl-3,7-dimethyloctanamide (2). Yield: 86%; a white solid, mp 44−46 °C. ^{1}H NMR ($CDCl_3$, 400 MHz): δ 0.86 (d, 6H, J = 6.4 Hz), 0.93 (d, 3H, J = 5.8 Hz), 1.14−1.31 (m, 6H), 1.50−1.53 (h, 1H, J = 6.4 Hz), 1.95−1.97 (m, 2H), 2.20−2.23 (m, 2H), 4.05−4.06 (d, 2H, J = 2.9 Hz), 5.71 (s, 1H). ^{13}C NMR ($CDCl_3$, 100 MHz): δ 19.61, 22.58, 22.65, 24.64, 27.88, 29.05, 30.77, 37.00, 39.00, 44.23, 71.46, 77.31, 172.30. IR (KBr): 3229, 3077, 2928, 1637, 1550, 1421, 1246, 1030, 723 cm^{-1}. $[\alpha]_D$ (c = 0.41 g/dL, $CHCl_3$): +0.25°. HRMS: calcd for $C_{13}H_{23}NO$ (*m/z*), 209.1780; found, 209.1781.

Polymerization. The (co)polymerization was carried out by using (nbd)Rh$^+$[(η^6-C_6H_5)B$^-$(C_6H_5)$_3$] as a initiator in dry THF under the following conditions: [monomer]$_{total}$ = 2.0 M, [catalyst] = 20 mM, 1 h, 30 °C. The resultant solution was poured into methanol to precipitate the (co)polymers. This precipitation procedure was carried out using ether for poly-

(**1b**), poly(**1c**). and poly(**1d**) and hexane for poly(**1a**) and poly(**1e**). The resultant polymers were collected, filtered, and dried under reduced pressure.

Acknowledgment. The authors thank Dr. M. Fujiki and Dr. M. Motonaga at NTT Basic Research Laboratories, Assistant Professor F. Sanda at Tokyo Institute of Technology, Dr. K. Naka and Professor Y. Chujo at Kyoto University for the GPC measurements, and Dr. H. Ohkita and Professor S. Ito at Kyoto University for the measurements of the temperature-variable UV−visible spectra. The authors are indebted to Professor S. Kimura at Kyoto University for permission for the use of a CD spectropolarimeter and also for his many valuable suggestions.

Supporting Information Available: Tables showing solubility of the homopolymers and data for the copolymers of **1** with **2** and a figure showing the temperature dependence of the UV−visible spectra of poly(**1e**) in $CHCl_3$. This material is available free of charge via the Internet at http://pubs.acs.org.

References and Notes

(1) Schulz, G. E.; Schirmer, R. H. *Principles of Protein Structure*; Springer-Verlag: New York, 1979.
(2) Saenger, W. *Principles of Nucleic Acid Structure*; Springer-Verlag: New York, 1984.
(3) For the synthesis of helical polymers, see: (a) Pu, L. *Acta Polym.* **1997**, *48*, 116−141. (b) Rowan, A. E.; Nolte, R. J. M. *Angew. Chem., Int. Ed. Engl.* **1998**, *37*, 63−68. (c) Okamoto, Y.; Nakano, T. *Chem. Rev.* **1994**, *94*, 349−372. (d) Qin, M.; Bartus, J.; Vogl, O. *Macromol. Symp.* **1995**, *12*, 387−402. (e) Nolte, R. J. M. *Chem. Soc., Rev.* **1994**, 11−19. (f) Nakano, T.; Okamoto, Y. *Macromol. Chem. Phys.* **2000**, *21*, 603−612.
(4) (a) Green, M. M.; Andreola, C.; Muñoz, B.; Reidy, M. P.; Zero, K. *J. Am. Chem. Soc.* **1988**, *110*, 4063−4065. (b) Green, M. M.; Gross, R. A.; Schilling, F. C.; Peterson, N. C.; Sato, T.; Teramoto, A.; Cook, R.; Lifson, S. *Science* **1995**, *268*, 1860−1866. (c) Okamoto, Y.; Matsuda, M.; Nakano, T.; Yashima, E. *J. Polym. Sci., Part A: Polym. Chem.* **1994**, *32*, 309−315. (d) Maeda, K.; Matsuda, M.; Nakano, T.; Okamoto, Y. *Polym. J.* **1995**, *27*, 141−146. (e) Jha, S. K.; Cheon, K. S.; Green, M. M.; Selinger, J. V. *J. Am. Chem. Soc.* **1999**, *121*, 1665−1673.
(5) (a) Kamer, P. C. J.; Nolte, R. J. M.; Drenth, W. J. *J. Am. Chem. Soc.* **1988**, *110*, 6818−6825. (b) Deming, T. J.; Novak, B. M. *J. Am. Chem. Soc.* **1993**, *115*, 9107−9108. (c) Takei, F.; Yanai, K.; Onitsuka, K.; Takahashi, S. *Angew. Chem., Int. Ed. Engl.* **1996**, *35*, 1554−1555. (d) Ito, Y.; Ohara, T.; Shima, R.; Suginome, M. *J. Am. Chem. Soc.* **1996**, *118*, 9188−9189.
(6) (a) Vogel, O.; Corley, L. S. *Polym. Bull. (Berlin)* **1980**, *3*, 211−217. (b) Ute, K.; Hirose, K.; Kashimoto, H.; Hatada, K.; Vogel, O. *J. Am. Chem. Soc.* **1991**, *113*, 6305−6306.
(7) Okamoto, Y.; Susuki, K.; Ohta, K.; Hatada, K.; Yuki, H. *J. Am. Chem. Soc.* **1979**, *101*, 4763−4764.
(8) Fujiki, M. *J. Am. Chem. Soc.* **1994**, *116*, 11976−11981.
(9) (a) Ciardelli, F.; Lanzillo, S.; Pieroni, O. *Macromolecules* **1974**, *7*, 174−179. (b) Tang, B. Z.; Kotera, N. *Macromolecules* **1989**, *22*, 4388−4390. (c) Yamaguchi, M.; Omata, K.; Hirama, M. *Chem. Lett.* **1992**, 2261−2262. (d) Kishimoto, Y.; Itou, M.; Miyatake, T.; Ikariya, T.; Noyori, R. *Macromolecules* **1995**, *28*, 6662−6666. (h) Nakako, H.; Nomura, R.; Tabata, M.; Masuda, T. *Macromolecules* **1999**, *32*, 2861−2864.
(10) (a) Aoki, T.; Kokai, M.; Shinohara, K.; Oikawa, E. *Chem. Lett.* **1993**, 2009−2012. (b) Yashima, E.; Huang, S.; Okamoto, Y. *J. Chem. Soc., Chem. Commun.* **1994**, 1811−1812. (c) Yashima, E.; Huang, S.; Matsushima, T.; Okamoto, Y. *Macromolecules* **1995**, *28*, 4184−4193. (d) Yashima, E.; Matsushima, T.; Okamoto, Y. *J. Am. Chem. Soc.* **1997**, *119*, 6345−6359. (e) Nakako, H.; Mayahara, Y.; Nomura, R.; Tabata, M.; Masuda, T. *Macromolecules* **2000**, *33*, 3978−3982.
(11) (a) Bouman, M. M.; Meijer, E. W. *Adv. Mater.* **1995**, *7*, 385−387. (b) Langeveld-Voss, B. M.; Janssen, R. A. J.; Christiaans, M. P. T.; Meskers, S. C. J.; Dekkers, H. P. J. M.; Meijer, E. W. *J. Am. Chem. Soc.* **1996**, *118*, 4908−4909.
(12) (a) Nakahira, T.; Lin, F.; Boon, C. T.; Karato, T.; Annaka, M.; Yoshikuni, M.; Iwabuchi, S. *Polym. J.* **1997**, *29*, 701−704. (b) Nakahira, T.; Fan, L.; Boon, C. T.; Fukada, Y.; Karato, T.; Annaka, M.; Yoshikuni, M. *Polym. J.* **1998**, *30*, 910−914.
(13) (a) Li, B. S.; Cheuk, K. K. L.; Salhi, F.; Lam, J. W. Y.; Cha, J. A. K.; Xiao, X.; Bai, C.; Tang, B. Z. *Nano Lett.* **2001**, *1*, 323−328. (b) Tang, B. Z. *Polym. News* **2001**, *26*, 262−272. See also references therein.
(14) Cornelissen, J. J. L. M.; Donners, J. J. J. M.; de Gelder, R.; Graswinckel, W. S.; Metselaar, G. A.; Rowan, A. E.; Sommerdijk, N. A. J. M.; Nolte, R. J. M. *Science* **2001**, *293*, 676−680.
(15) Nomura, R.; Tabei, J.; Masuda, T. *J. Am. Chem. Soc.* **2001**, *123*, 8430−8431.
(16) For recent reviews of the polymerization of substituted acetylenes, see: (a) Masuda, T. In *Catalysis in Precision Polymerization*; Kobayashi, S., Ed.; Wiley: Chichester, England, 1997; Chapter 2.4. (b) Masuda, T. In *Polymeric Material Encyclopedia*; Salamone, J. C., Ed.; CRC: New York, 1996, Vol. 1, pp 32−39. (c) Tabata, M.; Sone, T.; Sadahiro, Y. *Macromol. Chem. Phys.* **1999**, *200*, 265−282.
(17) (a) Lifson, S.; Andreola, C.; Peterson, N. C.; Green, M. M. *J. Am. Chem. Soc.* **1989**, *111*, 8850−8858. (b) Gu, H.; Nakamura, Y.; Sato, T.; Teramoto, A.; Green, M. M.; Andreola, C.; Peterson, N. C.; Lifson, S. *Macromolecules* **1995**, *28*, 1016−1024. (c) Okamoto, N.; Mukaida, F.; Gu, H.; Nakamura, Y.; Sato, T.; Teramoto, A.; Green, M. M. *Macromolecules* **1996**, *29*, 2878−2884. (d) Gu, H.; Nakamura, Y.; Sato, T.; Teramoto, A.; Green, M. M.; Jha, S. K.; Andreola, C.; Reidy, M. P. *Macromolecules* **1998**, *31*, 6362−6368. (e) Gu, H.; Sato, T.; Teramoto, A.; Varichon, L.; Green, M. M. *Polym. J.* **1997**, *29*, 77−84.
(18) Green, M. M.; Park, J.-W.; Sato, T.; Teramoto, A.; Lifson, S.; Selinger, R. L. B.; Selinger, J. V. *Angew. Chem., Int. Ed.* **1999**, *38*, 3138−3154.
(19) (a) Schrock, R. R.; Osborn, J. A *Inorg. Chem.* **1970**, *9*, 2339−2343. (b) Kishimoto, Y.; Itou, M.; Miyatake, T.; Ikariya, T.; Noyori, R. *Macromolecules* **1995**, *28*, 6662−6666.
(20) Since poly(**1d**) was very poorly soluble in $CDCl_3$, its ^{1}H NMR spectrum was measured in CD_3OD. In this solvent, poly(**1d**) displayed clear signals, and comparison of the integrated intensity of the signals due to the vinyl and NCH_2 protons proved that poly(**1d**) also possesses a quantitative cis content.
(21) Sharp ^{1}H NMR signals were attainable for poly(**1e**) and poly(**2**) when the spectra were recorded in the presence of a few drops of methanol-d_4 at high temperature (ca. 50 °C). The quantitative cis stereoregularity was confirmed by employing this technique.
(22) Norisuye, T. *Prog. Polym. Sci.* **1993**, *18*, 543−584.
(23) The monomer reactivity ratio of these copolymerizations was not determined due to the difficulty in the precise estimation of the copolymer compositions. Elemental analyses of the copolymers gave reasonable results only for the copolymers based on poly(**1a**) and poly(**1b**). The GPC trace detected by both polarimetric and RI detectors indicated that at least the homopolymer of achiral comonomer is not formed. Because of the absence of significant difference in the pendant structure between **1** and **2**, we assume that the chiral segment is probably dispersed randomly in the copolymer main chain.
(24) Temperature-variable UV−visible spectra of poly(**1e**) in $CHCl_3$ are illustrated in the Supporting Information.
(25) Nakako, H.; Nomura, R.; Masuda, T. *Macromolecules* **2001**, *34*, 1496−1502.
(26) Although an attempt was made to calculate the thermodynamic parameters for poly(**1e**), the calculation contained very large experimental errors and did not give reasonable values because, as shown in the Supporting Information, the conformational change of poly(**1e**) occurs in a very narrow temperature range. However, the temperature dependence of the UV−visible spectra of poly(**1e**) shows that there are very large, negative entropy changes for the process from the disordered to the ordered conformation.
(27) Nomura, R.; Fukushima, Y.; Nakako, H.; Masuda, T. *J. Am. Chem. Soc.* **2000**, *122*, 8830−8836.
(28) ΔG_r of poly(propiolic esters) is readily calculated by ^{1}H NMR spectra. See ref 27.
(29) Chan, K.-K.; Cohen, N.; De Noble, J. P.; Specian, A. C., Jr.; Saucy, G. *J. Org. Chem.* **1976**, *41*, 3497−3496.

MA0117155